

Exact gravity field for polyhedrons with polynomial density contrasts of arbitrary orders

Zhengyong Ren¹, Chaojian Chen^{1,2,*}, Yiyuan Zhong¹, Huang Chen¹,
Thomas Kalscheuer³, Hansruedi Maurer², Jingtian Tang^{1*}, Xiangyun Hu⁴

¹School of Geosciences and Info-Physics, Central South University, Changsha, Hunan, China.

²Department of Earth Sciences, Institute of Geophysics, ETH Zurich, Zurich, Switzerland.

³Department of Earth Sciences, Uppsala University, Uppsala, Sweden.

⁴Institute of Geophysics and Geomatics, Chinese University of Geoscience, Wuhan, Hubei, China.

Key Points:

- Anomaly mass target is represented by a set of polyhedral mass elements
- Density contrast is a polynomial function of arbitrary orders which can simultaneously vary in both horizontal and vertical directions
- Exact solutions of gravity fields are singularity-free

Corresponding author: Chaojian Chen, chenchaojian@csu.edu.cn

Corresponding author: Jingtian Tang, jttang@csu.edu.cn

Abstract

Computing gravity field of a mass body is a core routine to image anomalous density structures in the Earth. In this study, we report the existence of analytical routines to accurately compute the gravity potential and gravity field of a general polyhedral mass body. The density contrasts in the polyhedral body can be general polynomial functions up to arbitrary non-negative orders and also can vary in both horizontal and vertical directions. The newly derived analytical expressions of gravity fields are also singularity-free which means that observation sites can have arbitrary geometric relationships with polyhedral mass bodies. One synthetic prismatic body with different density contrasts is used to verify the accuracies of our new closed-form solutions. Excellent agreements are obtained among our solutions and other published solutions. Our work is the first-of-its kind to completely answer the fundamental question on existence of analytic solutions of gravitational field for general mass bodies. It may put an end of searching closed-form solutions in gravity surveying.

1 Introduction

Gravity data sets can be measured by gravimeters installed at land-based stations, on airplanes and ships, and even on satellites. Due to rapid developments of high precise gravimeters and financial invests, a large amount of gravity data sets are available to explore the minerals in the shallow surfaces, to investigate regional structures in the upper crust, even to image the density distributions in the mantle [Hautmann *et al.*, 2013; Panet *et al.*, 2014; Ye *et al.*, 2016; Martinez *et al.*, 2013]. To effectively extract anomalous density structures from measured gravity data sets, there is an urgent demand to develop routines aiming to forward compute accurately gravity fields for a given mass body [Barnett, 1976; Hofmann-Wellenhof and Moritz, 2006; Ren *et al.*, 2017a].

The analytical expression (or closed-form solution) for a polyhedral mass body is the routine of choice as it not only can well approximates complicated mass bodies in the Earth, but also offers ultimate accuracies. Since 1950s, intensive studies have been devoted to search closed-form formulae of gravity field for a polyhedral mass body with polynomial density contrasts as polynomial density contrasts can easily approximate the complicated mass density contributions in the Earth. For low order polynomial cases, a large amount of closed-form solutions were derived, such as the constant case [Paul, 1974; Barnett, 1976; Okabe, 1979; Holstein and Ketteridge, 1996; Holstein *et al.*, 1999;

Tsoulis and Petrovi, 2001; *Holstein*, 2002; *Tsoulis*, 2012], the linear case [*Wilton et al.*, 1984; *Holstein*, 2003; *Hamayun et al.*, 2009; *D’Urso*, 2014a; *Ren et al.*, 2017b], as well as the quadratic and cubic cases [*D’Urso and Trotta*, 2017; *Ren et al.*, 2018a,b]. However, density contrasts in the realistic Earth generally have more complicated distributions than those described by low order polynomials. For instance, exogenetic and endogenetic processes in the earth generally can change the mass density structures of the crust and mantle into three dimensional structures whose densities can vary both in horizontal and vertical directions [*Martin-Atienza and Garcia-Abdeslem*, 1999]. Therefore, it is more reasonable to consider a general density contrast of polynomial forms (of arbitrary orders) to more better approximate the true complicated density contrasts of the Earth.

In very recent years, several efforts have been paid to address above issues. For a prism, *Jiang et al.* [2017], *Karcol* [2018] and *Fukushima* [2018] successfully find closed-form solutions of gravity field for density contrast varying along depth by following a polynomial function of arbitrary orders. For a prism, *Zhang and Jiang* [2017] derived closed-form solutions of gravity field for density contrast varying both in horizontal and vertical directions and following polynomial functions of arbitrary orders. For a polyhedral prism, *Chen et al.* [2018] derived closed-form solutions of vertical gravity field with vertical polynomial density contrast up to arbitrary orders. A logic and theoretically important step is to find closed-form solutions of gravity field for a polyhedral body with arbitrary order polynomial density contrasts, which has not been addressed yet so far.

This study reports our latest finding which has successfully addressed above step. We find analytic formulae of both gravity potential and gravity field for a polyhedral body with polynomial density contrast up to arbitrary orders. The density contrasts in the polyhedral body can simultaneously vary in both horizontal and vertical directions. We use two synthetic models to verify accuracies of the new analytic formulae.

2 Theory and new analytic formulae

Let us adopt a right-handed Cartesian coordinate system where x -axis, y -axis are horizontally directed, and positive z -axis is vertically downward. For a polyhedral mass body H , gravity potential (ϕ) and gravity field (\mathbf{g}) at an observation site \mathbf{r}' are [*Blakely*,

1996]:

$$\phi(\mathbf{r}') = G \iiint_H \frac{\lambda(\mathbf{r})}{R} dv, \quad (1)$$

$$\mathbf{g}(\mathbf{r}') = \nabla_{\mathbf{r}'} \phi(\mathbf{r}') = G \iiint_H \lambda(\mathbf{r}) \nabla_{\mathbf{r}'} \frac{1}{R} dv, \quad (2)$$

where $G = 6.673 \times 10^{-11} \text{ m}^3 \text{ kg}^{-1} \text{ s}^{-2}$ is the gravitational constant, and $R = |\mathbf{r} - \mathbf{r}'|$ is the distance from the observation site \mathbf{r}' to a running integral point \mathbf{r} in body H , with $\mathbf{r} \in H$. The density contrast in the polyhedral body is denoted by $\lambda(\mathbf{r})$, which is a polynomial function varying in both horizontal and vertical directions:

$$\lambda(\mathbf{r}) = \sum_{p=0}^n \sum_{q=0}^{n-p} \sum_{t=0}^{n-(p+q)} a_{pqt} x^p y^q z^t, \quad (3)$$

where a_{pqt} is the constant coefficient which can be estimated by fitting measured field data sets, etc, from borehole [Blakely, 1996]. Non-negative integer n is the order of the polynomial function ($n \geq 0$). Non-negative integers p, q, t are three suborders along x -, y - and z -directions, respectively ($0 \leq p + q + t \leq n$).

Seeking for simplicity, we first move the observation site \mathbf{r}' to be the origin of the Cartesian coordinate system, that is $\mathbf{r}' = (0, 0, 0)$. After repeatedly using integration by parts, we finally obtain following formulae for both ϕ and \mathbf{g} :

$$\phi(\mathbf{r}') = G \sum_{p=0}^n \sum_{q=0}^{n-p} \sum_{t=0}^{n-(p+q)} a_{pqt} \phi(p, q, t), \quad (4)$$

$$\mathbf{g}(\mathbf{r}') = -G \sum_{p=0}^n \sum_{q=0}^{n-p} \sum_{t=0}^{n-(p+q)} a_{pqt} \mathbf{g}(p, q, t), \quad (5)$$

where

$$\phi(p, q, t) = \begin{cases} \sum_{i=1}^N (\hat{\mathbf{n}}_i \cdot \hat{\mathbf{x}}) I_s(p-1, q, t, 1) - (p-1) \cdot I_v(p-2, q, t, 1), & p \geq 2, \\ \sum_{i=1}^N (\hat{\mathbf{n}}_i \cdot \hat{\mathbf{x}}) I_s(0, q, t, 1), & p = 1, \\ I_v(0, q, t, -1), & p = 0, \end{cases}, \quad (6)$$

$$\mathbf{g}(p, q, t) = \sum_{i=1}^N \hat{\mathbf{n}}_i I_s(p, q, t, -1) - p \cdot \phi(p-1, q, t) \hat{\mathbf{x}} - q \cdot \phi(p, q-1, t) \hat{\mathbf{y}} - t \cdot \phi(p, q, t-1) \hat{\mathbf{z}}, \quad (7)$$

where N is the number of polygonal surfaces of the polyhedral body H , and $\hat{\mathbf{n}}_i$ is the outward normal vector of the i -th polygonal facet ∂H_i . The unit vectors along x -, y -, and z -directions are denoted by $\hat{\mathbf{x}}$, $\hat{\mathbf{y}}$, $\hat{\mathbf{z}}$, respectively. Symbols I_v and I_s represent the volume integrals and surface integrals, $I_v(a, b, c, w) = \iiint_H x^a y^b z^c R^w dv$, $I_s(\alpha, \beta, \gamma, \delta) = \iint_{\partial H_i} x^\alpha y^\beta z^\gamma R^\delta ds$, respectively, where $a, b, c, w, \alpha, \beta, \gamma, \delta$ are integer indices. Analytical expressions for I_v and I_s are listed in Text S1 of the supporting information.

Table 1. Comparison of our formula to other closed-form solutions of a polyhedral body for gravity potential (ϕ), and/or gravity field (\mathbf{g}). Symbol $-$ represents singularity, and symbol \checkmark indicates singularity-free.

Maxinium order	Singularity	Components	References
	free		
Constant	$-$	g_z	<i>Paul</i> [1974]; <i>Barnett</i> [1976]
Constant	$-$	\mathbf{g}	<i>Okabe</i> [1979]
Constant	\checkmark	\mathbf{g}	<i>Pohanka</i> [1988]; <i>Holstein and Ketteridge</i> [1996] <i>Hansen</i> [1999]; <i>Holstein et al.</i> [1999] <i>Tsoulis and Petrovi</i> [2001]; <i>Conway</i> [2015]
Constant	\checkmark	ϕ, \mathbf{g}	<i>Holstein</i> [2002] <i>Petrović</i> [1996]; <i>Tsoulis</i> [2012] <i>D’Urso</i> [2013, 2014a]
Linear	\checkmark	ϕ	<i>Hamayun et al.</i> [2009]
Linear	\checkmark	\mathbf{g}	<i>Pohanka</i> [1998]; <i>Hansen</i> [1999]
Linear	\checkmark	ϕ, \mathbf{g}	<i>Ren et al.</i> [2017b] <i>Holstein</i> [2003]; <i>D’Urso</i> [2014b]
Cubic order	\checkmark	ϕ, \mathbf{g}	<i>D’Urso and Trotta</i> [2017]; <i>Ren et al.</i> [2018b]
Arbitrary order	\checkmark	ϕ, \mathbf{g}	This study

During last 44 years, intensive studies were conducted to derive the closed-form solutions of gravity field for a polyhedral body. For reader’s convenience, we have listed these solutions in Table (1). Seen from this table, it is clear that our work unifies previous results.

3 Accuracy validation

A uniform prismatic body (see Figure 1) with density contrast of $\lambda(\mathbf{r}) = 2670 \text{ kg/m}^3$ is tested to verify the accuracies of our closed-form solutions. This model is taken from previous study [*Garcia-Abdeslem*, 2005] which has a size of $x = [10 \text{ km}, 20 \text{ km}]$, $y = [10 \text{ km}, 20 \text{ km}]$ and $z = [0 \text{ km}, 8 \text{ km}]$. Sixteen observations sites are equally spaced along a profile from $x = 0 \text{ km}$ to $x = 15 \text{ km}$, with $y = 15 \text{ km}$ and $z = 0 \text{ km}$. The gravity po-

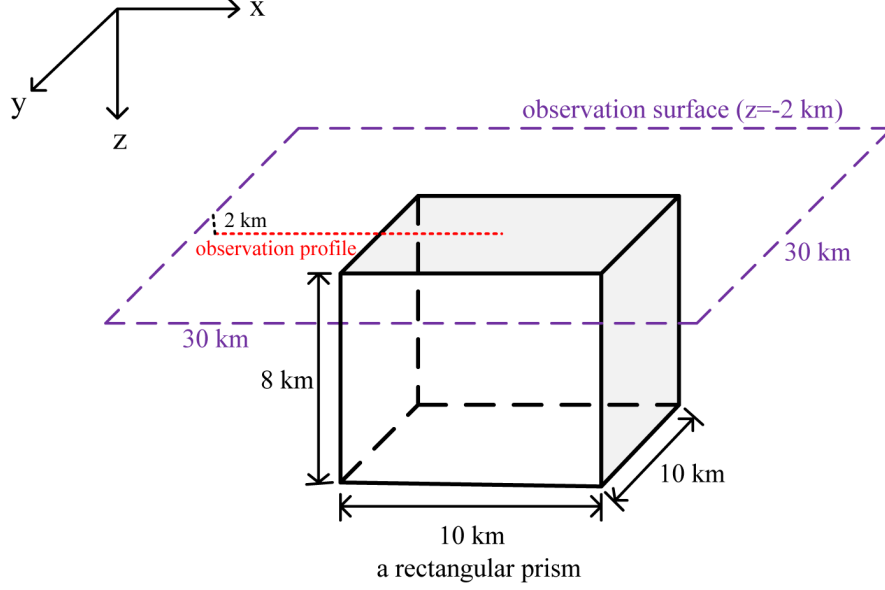


Figure 1. Illustration of the tested rectangular prism. Dashed line in red color represents the observation site which lies on the surface of the prism. The purple line represents the horizontal observation surface with $z = -2$ km.

tentials (ϕ) and vertical gravity fields (g_z) are calculated by four different methods, which are *Nagy et al.* [2000]’s analytical method (singularity-free formulae derived for a homogeneous prismatic body), *Tsoulis* [2012]’s analytical method (singularity-free formulae designed for a polyhedral body), high-order Gaussian numerical quadrature method with $512 \times 512 \times 512$ quadrature points [*Davis and Rabinowitz*, 1984] (working for a polyhedral body but with singularity), and our new formulae (singularity-free formulae designed for a polyhedral body).

Tables (2) and (3) show the gravity potentials and the vertical gravity fields computed by these four methods. When observation sites are outside the rectangular prism with x -coordinates ranging from 0 km to 9 km where no singularities exist, four solutions agree well with each other. The solutions of our and *Nagy et al.* [2000]’s formulae are identical up to the 13th significant digit, which are at the 7th significant digit between our formula and *Tsoulis* [2012]’s formula, and 11th significant digit between our formula and the high-order Gaussian quadrature rule. When observation sites locate on edge or surface of the prism with x -coordinates ranging from 10 km to 15 km where mathematic singularities exist, the high-order Gaussian quadrature with 134,217,728 quadrature points

cannot produce desired gravity fields. The relative errors between our solutions and high-order Gaussian quadrature rule's solutions are approximately $10^{-2}\%$ for gravity potential and $10^{-1}\%$ for vertical gravity field, respectively. Solutions of these three singularity-free analytical formulae still agree well with each other. Relative errors of our formulae referring to *Nagy et al.* [2000]'s formulae are less than $10^{-13}\%$ both for gravity potential and vertical gravity field. The relative errors are about $10^{-7}\%$ by referring to *Tsouliis* [2012]'s solutions, which suggests our solutions and *Nagy et al.* [2000]'s solutions maybe more accurate than *Tsouliis* [2012]'s solutions.

Table 2. Comparison of computed gravity potential (ϕ) by our new formula, *Nagy et al.* [2000]’s formula, *Tsoulis* [2012]’s formula and the high-order Gauss quadrature rule [*Davis and Rabinowitz*, 1984]. The observation sites are equally spaced on the profile from $x = 0$ km to $x = 15$ km with $y = 15$ km and $z = 0$ km. Differences of later three solutions referring to our closed-form solutions are marked by bold face.

ϕ (m ² s ⁻²) on the observation profile ($y = 15$ km and $z = 0$ m)				
x (km)	Our solution	<i>Nagy et al.</i> [2000]’s solution	<i>Tsoulis</i> [2012]’s solution	Gauss quadrature rule’s solution
0	9.213370778767388E+0	9.2133707787673 96 E+0	9.2133 69100056041 E+0	9.2133707787663 66 E+0
1	9.824631495073580E+0	9.8246314950735 76 E+0	9.82463 0015757330 E+0	9.82463149507 4603 E+0
2	1.051797364599913E+1	1.0517973645999 04 E+1	1.051797 237193737 E+1	1.051797364 600060 E+1
3	1.130972911860967E+1	1.1309729118609 65 E+1	1.130972 805682759 E+1	1.130972911861 287 E+1
4	1.222032550160522E+1	1.2220325501605 19 E+1	1.222032 466058624 E+1	1.222032550160 315 E+1
5	1.327538330028535E+1	1.3275383300285 37 E+1	1.327538 269034185 E+1	1.327538330028 375 E+1
6	1.450701005685137E+1	1.4507010056851 29 E+1	1.45070 0969058767 E+1	1.450701005685 489 E+1
7	1.595517547999473E+1	1.5955175479994 65 E+1	1.5955175 37286842 E+1	1.595517547999 217 E+1
8	1.766884275902838E+1	1.7668842759028 33 E+1	1.766884 292999224 E+1	1.766884275902 748 E+1
9	1.970619558083274E+1	1.9706195580832 89 E+1	1.97061 9605299300 E+1	1.970619558083 330 E+1
10	2.213300296314875E+1	2.2133002963148 86 E+1	2.213300 307117277 E+1	2.213 298105404876 E+1
11	2.445867695151962E+1	2.4458676951519 59 E+1	2.445867 667261200 E+1	2.44586 3325909497 E+1
12	2.618973014389963E+1	2.6189730143899 57 E+1	2.6189730 09759514 E+1	2.61896 8115907312 E+1
13	2.738306438467226E+1	2.7383064384672 19 E+1	2.7383064 50143388 E+1	2.738301 380637997 E+1
14	2.808152004294769E+1	2.808152004294769E+1	2.8081520 25629653 E+1	2.8081 46845667066 E+1
15	2.831139474536049E+1	2.8311394745360 48 E+1	2.8311394 99069494 E+1	2.83113 3673809870 E+1

Table 3. Similar to Table 2, but for the vertical gravity field (g_z).

g_z (m s ⁻²) on the observation profile ($y = 15$ km and $z = 0$ m)				
x (km)	Our solution	<i>Nagy et al.</i> [2000]’s solution	<i>Tsoulis</i> [2012]’s solution	Gauss quadrature rule’s solution
0	1.569077805220523E-4	1.569077805220 415 E-4	1.569077 9172288047 E-4	1.569077805220 810 E-4
1	1.903530880423478E-4	1.903530880423 529 E-4	1.90353 10163066231 E-4	1.903530880423 669 E-4
2	2.336177366177579E-4	2.336177366177 611 E-4	2.336177 5329451025 E-4	2.336177366177 468 E-4
3	2.903939376743299E-4	2.9039393767432 63 E-4	2.903939 5840403946 E-4	2.90393937674 2514 E-4
4	3.660760399102218E-4	3.6607603991022 50 E-4	3.660760 6604248237 E-4	3.6607603991022 69 E-4
5	4.687144103570855E-4	4.6871441035708 56 E-4	4.687144 4381616444 E-4	4.6871441035708 09 E-4
6	6.106620777037364E-4	6.1066207770373 54 E-4	6.10662 12129571923 E-4	6.106620777037 133 E-4
7	8.116930153767311E-4	8.1169301537673 53 E-4	8.116930 7331926445 E-4	8.116930153767 775 E-4
8	1.106000581484408E-3	1.1060005814844 15 E-3	1.106000 6604360253 E-3	1.106000581484 175 E-3
9	1.564054962964779E-3	1.5640549629647 81 E-3	1.56405 50746145116 E-3	1.564054962964 430 E-3
10	2.500274605795732E-3	2.5002746057957 36 E-3	2.500274 9088856207 E-3	2.496489446288155 E-3
11	3.428396737487712E-3	3.4283967374877 04 E-3	3.42839 72314397134 E-3	3.420841483175205 E-3
12	3.861374139996904E-3	3.86137413999690 1 E-3	3.861374 6648569073 E-3	3.853287806877850 E-3
13	4.111139415564093E-3	4.11113941556409 7 E-3	4.111139 9582535370 E-3	4.102938786513448 E-3
14	4.243541894555503E-3	4.24354189455550 5 E-3	4.24354 24466964718 E-3	4.235268733626918 E-3
15	4.285156168585589E-3	4.2851561685855 95 E-3	4.285156 7236971821 E-3	4.276333953447218 E-3

In order to test performances of our closed-form solutions for varying density contrasts, the same prismatic body in Figure 1 is tested, but with quartic order density contrasts. The density contrast is mixed in both horizontal and vertical directions:

$$\lambda(\mathbf{r}) = x^2 y z, \quad (8)$$

where the density is in units of kg/m^3 and x, y, z are in units of km. Totally, a number of 256 observation sites are uniformly arranged at a plane with horizontal coordinates ranging from 0 km to 30 km in both x and y directions. The measuring plane has a vertical offset of $z = -2$ km to the top surface of the prism, which means there are no singularities in the gravity field vector. Due to no closed-form solutions available, we have to use the high-order Gaussian quadrature rule with $512 \times 512 \times 512$ quadrature points [Davis and Rabinowitz, 1984] to compute the reference solutions. Because the gravity field on this measuring plane is regular, therefore, the high-order Gaussian quadrature could generate reliable reference solutions.

We compare the gravity fields computed by both our formula and the high-order Gaussian quadrature rule on this measuring plane, which are shown in Figure 2. As expected, excellent agreements are obtained for all the three components of the gravity fields. The relative errors between our solution and the high-order Gaussian quadrature rule's solution are less than $10^{-10}\%$. As presented in Table 4, the maximum absolute residual of the computed gravity field is $1.969 \times 10^{-12} \text{ ms}^{-2}$, which is far less than the instrument precision of typical gravimeters used in current gravity surveys (such as approximately $5 \cdot 10^{-8} \text{ ms}^{-2}$ for CG-5 gravimeter [Reudink et al., 2014]). The mean square residuals are less than $3.507 \times 10^{-14} \text{ ms}^{-2}$. These almost negligible residuals verify the high accuracy of our new formula for the case of varying density contrasts. However, happening to almost all analytical formulae [Holstein, 2003; Ren et al., 2018a; Jiang et al., 2018; Chen et al., 2018], phenomenon of numerical instability still exist in our new formula when the distance between the observation site and the polyhedral mass body beyond a critical level. This phenomenon is caused by the limited machine precision to present the real number in the calculation, which can be resolved by using longer bits such as 128 bits to represent real numbers or equivalent real number representation methods.

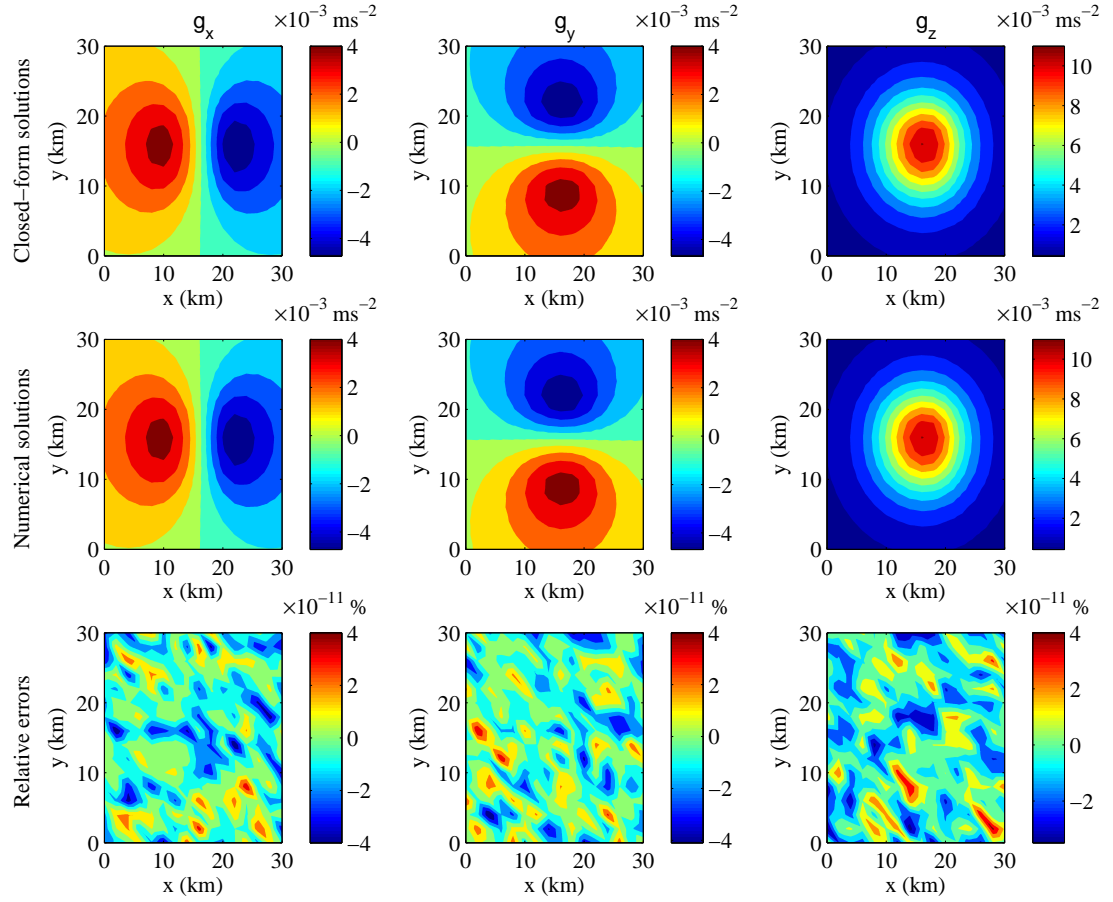


Figure 2. Comparison of computed three components of gravity fields (g_x, g_y, g_z) calculated by both our formulae (upper row) and the high-order Gaussian numerical quadrature rule with $512 \times 512 \times 512$ quadrature points (middle row) for the case the measuring profile is above the prismatic body. The relative errors are shown in the bottom row.

Table 4. Residuals statistics between our solutions and those from the high-order Gaussian quadrature rule with $512 \times 512 \times 512$ quadrature points for gravity fields shown in Figure 2.

	$g_x(\text{ms}^{-2})$	$g_y(\text{ms}^{-2})$	$g_z(\text{ms}^{-2})$
Max	1.890×10^{-12}	1.069×10^{-12}	1.969×10^{-12}
Min	-1.230×10^{-12}	-9.996×10^{-13}	-2.903×10^{-12}
Mean	2.005×10^{-14}	1.881×10^{-14}	3.507×10^{-14}

4 Discussion and Conclusions

We report the existence of closed-form solutions of gravity field for a polyhedral body with general density contrasts. The density contrast is represented by a polynomial function of arbitrary orders. This polynomial density function can vary in both horizontal and vertical directions. Our closed-form solutions are singularity-free which means that the observation sites can be located at any place outside, inside, on the vertices of and at the edges of the polyhedral bodies. A synthetic prismatic body with different density contrasts are tested to verify our formula's accuracies. Excellent agreements between our new solutions and other solutions verify the capability of our new findings to accurately calculate gravity fields. With our new findings, the door of room containing closed-form solutions for polyhedral bodies with polynomial density functions can be closed.

Acknowledgments

This work was financially supported by the National Science Foundation of China (41574120), a joint China-Sweden mobility project (STINT-NSFC, 4171101400), and the China Scholarship Council Foundation (201806370223), the National Basic Research Program of China (973-2015CB060200).

References

- Barnett, C. T. (1976), Theoretical modeling of the magnetic and gravitational fields of an arbitrarily shaped three dimensional body, *Geophysics*, *41*(6), 1353–1364.
- Blakely, R. J. (1996), *Potential Theory in Gravity and Magnetic Applications*, Cambridge University Press.
- Chen, C., Z. Ren, K. Pan, J. Tang, T. Kalscheuer, H. Maurer, Y. Sun, and Y. Li (2018), Exact solutions of the vertical gravitational anomaly for a polyhedral prism with vertical polynomial density contrast of arbitrary orders, *Geophysical Journal International*, *214*(3), 2115–2132.
- Conway, J. T. (2015), Analytical solution from vector potentials for the gravitational field of a general polyhedron, *Celestial Mechanics and Dynamical Astronomy*, *121*(1), 17–38.
- Davis, P. J., and P. Rabinowitz (1984), *Methods of Numerical Integration (Second Edition)*, Academic Press, San Diego.

- D’Urso, M. G. (2013), On the evaluation of the gravity effects of polyhedral bodies and a consistent treatment of related singularities, *Journal of Geodesy*, 87(3), 239–252.
- D’Urso, M. G. (2014a), Analytical computation of gravity effects for polyhedral bodies, *Journal of Geodesy*, 88(1), 13–29.
- D’Urso, M. G. (2014b), Gravity effects of polyhedral bodies with linearly varying density, *Celestial Mechanics and Dynamical Astronomy*, 120(4), 349–372.
- D’Urso, M. G., and S. Trotta (2017), Gravity anomaly of polyhedral bodies having a polynomial density contrast, *Surveys in Geophysics*, 38(4), 781–832.
- Fukushima, T. (2018), Recursive computation of gravitational field of a right rectangular parallelepiped with density varying vertically by following an arbitrary degree polynomial, *Geophysical Journal International*, 215(2), 864–879.
- Garcia-Abdeslem, J. (2005), The gravitational attraction of a right rectangular prism with density varying with depth following a cubic polynomial, *Geophysics*, 70(6), J39–J42.
- Hamayun, I. Prutkin, and R. Tenzer (2009), The optimum expression for the gravitational potential of polyhedral bodies having a linearly varying density distribution, *Journal of Geodesy*, 83(12), 1163–1170.
- Hansen, R. O. (1999), An analytical expression for the gravity field of a polyhedral body with linearly varying density, *Geophysics*, 64(1), 75–77.
- Hautmann, S., A. G. Camacho, J. Gottsmann, H. M. Odbert, and R. T. Syers (2013), The shallow structure beneath montserrat (west indies) from new bouguer gravity data, *Geophysical Research Letters*, 40(19), 5113–5118.
- Hofmann-Wellenhof, B., and H. Moritz (2006), *Physical Geodesy*, Springer.
- Holstein, H. (2002), Gravimagnetic similarity in anomaly formulas for uniform polyhedra, *Geophysics*, 67(4), 1126–1133.
- Holstein, H. (2003), Gravimagnetic anomaly formulas for polyhedra of spatially linear media, *Geophysics*, 68(1), 157–167.
- Holstein, H., and B. Ketteridge (1996), Gravimetric analysis of uniform polyhedra, *Geophysics*, 61(2), 357–364.
- Holstein, H., P. Schürholz, A. J. Starr, and M. Chakraborty (1999), Comparison of gravimetric formulas for uniform polyhedra, *Geophysics*, 64(5), 1438–1446.

- Jiang, L., J. Zhang, and Z. Feng (2017), A versatile solution for the gravity anomaly of 3D prism-meshed bodies with depth-dependent density contrast, *Geophysics*, *82*(4), G77–G86.
- Jiang, L., J. Liu, J. Zhang, and Z. Feng (2018), Analytic expressions for the gravity gradient tensor of 3D prisms with depth-dependent density, *Surveys in Geophysics*, *39*(3), 337–363.
- Karcol, R. (2018), The gravitational potential and its derivatives of a right rectangular prism with depth-dependent density following an n-th degree polynomial, *Studia Geophysica et Geodaetica*, *62*(3), 427–449.
- Martin-Atienza, B., and J. Garcia-Abdeslem (1999), 2-D gravity modeling with analytically defined geometry and quadratic polynomial density functions, *Geophysics*, *64*(6), 1730–1734.
- Martinez, C., Y. Li, R. Krahenbuhl, and M. A. Braga (2013), 3D inversion of airborne gravity gradiometry data in mineral exploration: A case study in the quadriltero ferrifero, brazil, *Geophysics*, *78*(1), B1–B11.
- Nagy, D., G. Papp, and J. Benedek (2000), The gravitational potential and its derivatives for the prism, *Journal of Geodesy*, *74*(7-8), 552–560.
- Okabe, M. (1979), Analytical expressions for gravity anomalies due to homogeneous polyhedral bodies and translations into magnetic anomalies, *Geophysics*, *44*(4), 730–741.
- Panet, I., G. Pajotmtivier, M. Grefflefftz, L. Mtivier, M. Diamant, and M. Mandeia (2014), Mapping the mass distribution of earth’s mantle using satellite-derived gravity gradients, *Nature Geoscience*, *7*(2), 131–135.
- Paul, M. K. (1974), The gravity effect of a homogeneous polyhedron for three-dimensional interpretation, *Pure and applied geophysics*, *112*(3), 553–561.
- Petrović, S. (1996), Determination of the potential of homogeneous polyhedral bodies using line integrals, *Journal of Geodesy*, *71*(1), 44–52.
- Pohanka, V. (1988), Optimum expression for computation of the gravity field of a homogeneous polyhedral body, *Geophysical Prospecting*, *36*(7), 733–751.
- Pohanka, V. (1998), Optimum expression for computation of the gravity field of a polyhedral body with linearly increasing density, *Geophysical Prospecting*, *46*(4), 391–404.

- Ren, Z., J. Tang, T. Kalscheuer, and H. Maurer (2017a), Fast 3-D large-scale gravity and magnetic modeling using unstructured grids and an adaptive multilevel fast multipole method, *Journal of Geophysical Research: Solid Earth*, *122*(1), 79–109.
- Ren, Z., C. Chen, K. Pan, T. Kalscheuer, H. Maurer, and J. Tang (2017b), Gravity anomalies of arbitrary 3D polyhedral bodies with horizontal and vertical mass contrasts, *Surveys in Geophysics*, *38*(2), 479–502.
- Ren, Z., Y. Zhong, C. Chen, J. Tang, T. Kalscheuer, H. Maurer, and Y. Li (2018a), Gravity gradient tensor of arbitrary 3D polyhedral bodies with up to third-order polynomial horizontal and vertical mass contrasts, *Surveys in Geophysics*, *39*(5), 901–935.
- Ren, Z., Y. Zhong, C. Chen, J. Tang, and K. Pan (2018b), Gravity anomalies of arbitrary 3D polyhedral bodies with horizontal and vertical mass contrasts up to cubic order, *Geophysics*, *83*(1), G1–G13.
- Reudink, R., R. Klees, O. Francis, J. Kusche, R. Schlesinger, A. Shabanloui, N. Sneeuw, and L. Timmen (2014), High tilt susceptibility of the Scintrex CG-5 relative gravimeters, *Journal of Geodesy*, *88*(6), 617–622.
- Tsoulis, D. (2012), Analytical computation of the full gravity tensor of a homogeneous arbitrarily shaped polyhedral source using line integrals, *Geophysics*, *77*(2), F1–F11.
- Tsoulis, D., and S. Petrovi (2001), On the singularities of the gravity field of a homogeneous polyhedral body, *Geophysics*, *66*(2), 535–539.
- Wilton, D., S. Rao, A. Glisson, D. Schaubert, O. Al-Bundak, and C. Butler (1984), Potential integrals for uniform and linear source distributions on polygonal and polyhedral domains, *IEEE Transactions on Antennas and Propagation*, *32*(3), 276–281.
- Ye, Z., R. Tenzer, N. Sneeuw, L. Liu, and F. Wild-Pfeiffer (2016), Generalized model for a moho inversion from gravity and vertical gravity-gradient data, *Geophysical Journal International*, *207*(1), 111–128.
- Zhang, J., and L. Jiang (2017), Analytical expressions for the gravitational vector field of a 3-D rectangular prism with density varying as an arbitrary-order polynomial function, *Geophysical Journal International*, *210*(2), 1176–1190.